Pseudospectral Modal Method for Computing Optical Waveguide Modes

Dawei Song and Ya Yan Lu

***Abstract*—For optical waveguides with high index-contrast and sharp corners, it is challenging to develop efficient, accurate and general full-vectorial mode solvers. The classical mode-matching method is capable of computing modes to high accuracy for waveguides with right-angle corners, but it is not convenient to implement when the waveguide has lossy components. Numerical variants of the mode-matching method, such as the Fourier modal method (as a mode solver), are simpler to implement. In this paper, a recently developed pseudospectral modal method (PSMM) for diffraction gratings is reformulated as a full-vectorial waveguide mode solver. As demonstrated in a number of examples, the method can be used to calculate waveguide modes to high accuracy, and it is relatively simple to implement.**

I. Introduction

In recent years, many novel optical waveguides have been designed and fabricated. Some of these waveguides such as photonic crystal fibers, have complicated micro-structures, while others such as silicon, plasmonic or hybrid plasmonic waveguides, have high index-contrast and possibly sharp corners. Numerical modeling of these new waveguides require advanced numerical methods with high efficiency and accuracy. The basic mathematical problem for an optical waveguide is to calculate its guided or leaky modes. This is usually formulated at a fixed frequency as a linear eigenvalue problem for computing the propagation constant β and the mode profile. Notice that for waveguides with lossy components (such as metals), the propagation constant β is complex. On the other hand, β is always complex for leaky modes even if the waveguide components are lossless.

Existing numerical methods for computing waveguide modes can be classified as linear and nonlinear methods. Linear methods, such as the finite difference method [1]–[4], the finite element method [5]–[8], and the multi-domain pseudospectral method [9]–[12], discretize the waveguide cross section and give rise to linear matrix eigenvalue problems. The linear methods are very natural, as they are closely related to the original eigenvalue problem for differential operators formulated on the plane perpendicular to the waveguide axis, and they also have the advantage of reducing the problem to standard matrix eigenvalue problems for which extensive numerical linear algebra tools are available. However, these methods typically produce very large matrices, and the corresponding matrix eigenvalue problems are not easy to solve.

A nonlinear method formulates the waveguide eigenvalue problem as

$$\mathbf{F}(\beta)\boldsymbol{x} = \mathbf{0}, \tag{1}$$

where $\mathbf{F}$ is a square matrix and β appears implicitly in the matrix $\mathbf{F}$. Compared with the matrices that appear in the linear methods, the matrix $\mathbf{F}$ above has a much smaller size. To find a mode from Eq. (1), we can determine β from the condition that $\mathbf{F}(\beta)$ is a singular matrix, then construct the electromagnetic field of the mode from the the corresponding non-zero vector $\boldsymbol{x}$. Existing nonlinear methods include the multipole method [13]–[16], the boundary integral equation (BIE) method [17]–[22], the mode-matching method [23]–[29], and numerical variants of the mode-matching method based on finite difference approximations [30] or Fourier series expansions [31], [32]. The multipole method is basically restricted to waveguides with circular inclusions. The BIE method is applicable to optical waveguides with piecewise constant refractive index profiles. It achieves high accuracy for waveguides with complicated microstructures [21] and sharp corners [22], but is somewhat complicated to implement. The mode-matching method and its numerical variants are only applicable to waveguides with vertical and horizontal interfaces, but they are relatively simple to implement and appear to be quite accurate. In a benchmark calculation for a silicon waveguide with a rectangular core [33], the mode-matching method and a variant based on Fourier series have outperformed all other methods.

The (analytic) mode-matching method and related numerical variants divide the transverse plane (perpendicular to the waveguide axis) into a number of regions where the refractive index depends only on one spatial variable, expand the electromagnetic field of a waveguide mode in one-dimensional (1D) modes of the region, and match the tangential field components along the boundaries of these regions. The mode-matching method [23]–[29] calculates the 1D modes analytically, and matches the field components by projection on a set of 1D modes. The numerical variants [30], [31] calculate the 1D modes by the finite-difference method or Fourier series expansions, then match the tangential field components pointwise or by their Fourier coefficients. It is important to note that the mode-matching method corresponds to the analytic modal method for conical diffraction gratings [34], and the finite-difference and Fourier-series variants correspond to the finite-difference modal method [35] and the Fourier modal method

This work was partially supported by the National Natural Science Foundation of China (Project No. 11301265) and the Research Grants Council of Hong Kong Special Administrative Region, China (Project No. CityU 102411).

D. Song is with the Department of Mathematics, Nanjing University of Aeronautics and Astronautics, Nanjing, Jiangsu, China (e-mail: dwsmath@nuaa.edu.cn).

Y. Y. Lu is with the Department of Mathematics, City University of Hong Kong, Kowloon, Hong Kong (e-mail: mayylu@cityu.edu.hk).

[31], respectively.

Recently, the pseudospectral modal method (PSMM) was developed for in-plane and conical diffraction grating problems [36]–[40]. The method has outperformed the standard Fourier modal method and a high order finite difference modal method [40]. In this paper, we extend the PSMM as a numerical variant of the mode-matching method for computing optical waveguide modes. We also include a coordinate stretching technique to increase the resolution near waveguide corners (as in the adaptive spatial resolution technique for the Fourier modal method [32], [41], [42]), and to extend the truncation domain without increasing the number of discretization points. The method is relatively simple to implement and highly accurate. A number of numerical examples are used to illustrate the performance of our method.

II. Mode-matching method

We consider optical waveguides characterized by a z-independent dielectric function $\varepsilon(x, y)$, where $\{x, y, z\}$ is a Cartesian coordinate system, z is the variable along the waveguide axis, x and y are the transverse variables. For clarity, we assume x and y are the horizontal and vertical variables, respectively. For time-harmonic waves that depend on time as $\exp(-i\omega t)$, where ω is the angular frequency, the governing equations are the following Maxwell's equations

$$\nabla \times \boldsymbol{E} = ik_0 \boldsymbol{H}, \quad \nabla \times \boldsymbol{H} = -ik_0 \varepsilon \boldsymbol{E}, \tag{2}$$

where k_0 is the free space wavenumber, $\boldsymbol{E}$ is the electric field and $\boldsymbol{H}$ is the magnetic field multiplied by the free space impedance. A waveguide mode is a special solution of Eq. (2), such that the z-dependence is $\exp(i\beta z)$ for a propagation constant β. In this paper, we only consider guided modes that decay to zero exponentially as $r = \sqrt{x^2 + y^2} \to \infty$.

The mode-matching method and its numerical variants are applicable to waveguides with only vertical or horizontal material interfaces. We assume the xy plane can be divided into $l_* + 1$ regions (vertical slices), given by $x < x_1$, $x_{l-1} < x < x_l$ for $2 \le l \le l_*$, and $x > x_{l_*}$, such that $\varepsilon(x, y) = \varepsilon_l(y)$ in the lth region. As an example, we have three regions shown in Fig. 1 for a rib waveguide. Of course, the method also works if the xy plane is divided into a number of horizontal slices in which ε depends only on x. The choice should be made to minimize the computation effort which is mainly related to the size of the matrix $\mathbf{F}$ in Eq. (1). For the rib waveguide, if horizontal slices are used, there will be four regions and three interfaces, and the matrix $\mathbf{F}$ will be larger.

In a region where the dielectric function ε depends only on y, it can be easily shown that the y components of the electromagnetic field satisfy separate Helmholtz equations

$$\frac{\partial^2 E_y}{\partial x^2} + \frac{\partial}{\partial y}\left[\frac{1}{\varepsilon}\frac{\partial(\varepsilon E_y)}{\partial y}\right] + \frac{\partial^2 E_y}{\partial z^2} + k_0^2 \varepsilon E_y = 0, \tag{3}$$

$$\frac{\partial^2 H_y}{\partial x^2} + \frac{\partial^2 H_y}{\partial y^2} + \frac{\partial^2 H_y}{\partial z^2} + k_0^2 \varepsilon H_y = 0. \tag{4}$$

General solutions for Eqs. (3) and (4) can be written down by the method of separation of variables (for εE_y and H_y, respectively). This leads to expansions of the electromagnetic field in terms of the vertical transverse electric (TE) and transverse magnetic (TM) modes. The governing equations for these 1D modes are

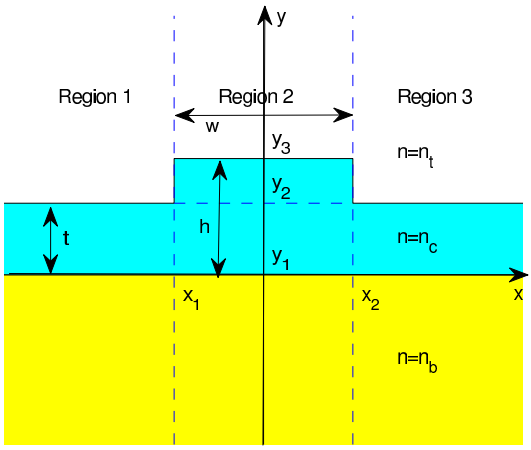

Fig. 1. Three regions of a rib waveguide given by $x < x_1$, $x_1 < x < x_2$ and $x > x_2$ respectively.

$$\varepsilon \frac{d}{dy}\left(\frac{1}{\varepsilon}\frac{d\phi}{dy}\right) + k_0^2 \varepsilon \phi = \hat{\delta}^2 \phi, \tag{5}$$

$$\frac{d^2\psi}{dy^2} + k_0^2 \varepsilon\, \psi = \hat{\nu}^2 \psi, \tag{6}$$

where ϕ and ψ are eigenfunctions (functions of z) for the TM and TE modes, respectively, $\hat{\delta}^2$ and $\hat{\nu}^2$ are the corresponding eigenvalues. If we truncate y to a finite interval (y_0, y_*) and impose the zero boundary conditions

$$\phi = \psi = 0 \quad \text{at} \quad y = y_0,\ y_*, \tag{7}$$

then the eigenvalue problems give rise to infinite sequences of eigenpairs. We denote these eigenfunctions and the eigenvalues by ϕ_j, $\hat{\delta}_j^2$, ψ_j, $\hat{\nu}_j^2$ for $j = 1, 2, 3, \ldots$

If the refractive index of the region is piecewise constant in y, the eigenvalue problems (5), (6) and (7) can be solved analytically, in the sense that the eigenfunctions are given analytically in each interval where ε is constant, but the eigenvalues are calculated by solving a transcendental equation numerically. For waveguides with lossy components, ε is complex in some part of the region, then the eigenvalues $\hat{\delta}^2$ and $\hat{\nu}^2$ are also complex. Since it is not easy to find all roots of a transcendental equation in the complex plane, the analytic mode-matching method is not so convenient to implement, at least for waveguides with lossy components. On the other hand, it is very simple to solve the eigenvalue problems (5), (6) and (7) numerically. A finite difference method was first used in [30]. In the Fourier modal method [31], the boundary condition (7) is replaced by a periodic condition, then the eigenvalue problems are solved by expanding the eigenfunctions in Fourier series.

Using the 1D modes, we can write down E_y and H_y in the

lth region as

$$E_y(x,y) = \frac{1}{\varepsilon_l(y)} \sum_{j=1}^{\infty} \hat{\delta}_j^2 \, \phi_j(y) \, U_j(x), \tag{8}$$

$$H_y(x,y) = \sum_{j=1}^{\infty} \hat{\nu}_j^2 \, \psi_j(y) \, V_j(x), \tag{9}$$

where

$$U_j(x) = a_j e^{i\delta_j(x-x_{l-1})} + b_j e^{-i\delta_j(x-x_l)}, \tag{10}$$

$$V_j(x) = c_j e^{i\nu_j(x-x_{l-1})} + d_j e^{-i\nu_j(x-x_l)}, \tag{11}$$

$$\delta_j = \sqrt{\hat{\delta}_j^2 - \beta^2}, \quad \nu_j = \sqrt{\hat{\nu}_j^2 - \beta^2}, \tag{12}$$

a_j, b_j, c_j and d_j are unknown coefficients. The complex square root in Eq. (12) is defined such that δ_j and ν_j are either real and positive or complex with positive imaginary parts. In the first and last regions, U_j and V_j must be modified to include only outgoing terms. That is, $a_j = c_j = 0$ for the first region ($x < x_1$) and $b_j = d_j = 0$ for the last region ($x > x_{l_*}$). The other four components of the electromagnetic field can also be expressed using the 1D modes and the functions U_j and V_j. The z components are given as

$$E_z(x,y) = i \sum_{j=1}^{\infty} \left[\frac{\beta}{\varepsilon_l(y)} \frac{d\phi_j(y)}{dy} U_j(x) - k_0 \psi_j(y) \frac{V_j(x)}{dx} \right], \tag{13}$$

$$H_z(x,y) = i \sum_{j=1}^{\infty} \left[\beta \frac{d\psi_j(y)}{dy} V_j(x) + k_0 \phi_j(y) \frac{dU_j(x)}{dx} \right]. \tag{14}$$

It is important to note that the 1D modes and the expansion coefficients are different in different regions. To explicitly indicate the quantities in the lth region, we could add a superscript (l). This leads to eigenfunctions $\phi_j^{(l)}$ and $\psi_j^{(l)}$, eigenvalues $\hat{\delta}_j^{(l)}$ and $\hat{\nu}_j^{(l)}$ (and related $\delta_j^{(l)}$ and $\nu_j^{(l)}$), and expansion coefficients $a_j^{(l)}$, $b_j^{(l)}$, $c_j^{(l)}$ and $d_j^{(l)}$.

With the mode expansions in each region, we can establish Eq. (1) by matching E_y, H_y, E_z and H_z on the vertical lines $x = x_l$ for $1 \le l \le l_*$. In the above, $\boldsymbol{x}$ is a column vector for $\boldsymbol{b}^{(1)}$, $\boldsymbol{d}^{(1)}$, $\boldsymbol{a}^{(l)}$, $\boldsymbol{b}^{(l)}$, $\boldsymbol{c}^{(l)}$, $\boldsymbol{d}^{(l)}$ ($2 \le l \le l_*$), $\boldsymbol{a}^{(l_*+1)}$ and $\boldsymbol{c}^{(l_*+1)}$, where $\boldsymbol{a}^{(l)}$ is the column vector for $a_j^{(l)}$, etc. For the analytic mode-matching method, the expansions (8), (9), (13) and (14) are first truncated to N terms, then the continuity conditions are imposed by inner products with a chosen set of 1D modes. In the finite-difference approach, the y variable is discretized by N points, then Eq. (1) is established by simply matching the four field components at these N points of y for each x_l, $1 \le l \le l_*$. In the Fourier modal method, Eq. (1) is obtained by matching the coefficients of N retained terms in the Fourier series.

III. Pseudospectral modal method

In this section, we present a PSMM for computing waveguide modes as an extension of the PSMM for conical diffraction of gratings [40]. Briefly, we use the Chebyshev pseudospectral method [37], [43] to calculate the 1D TE and TM modes, replace the expansions (8), (9), (13) and (14) by their numerical approximations, then point-match the four field components on the vertical lines at $x = x_l$ for $1 \le l \le l_*$ to establish the homogeneous linear system (1).

To match the field components on the vertical lines, it is necessary to use the same discretization points for y in all regions. For that purpose, we need to locate all horizontal interfaces which are assumed to be $y = y_p$ for $1 \le p < P$ satisfying $y_0 < y_1 < y_2 < ... < y_{P-1} < y_*$, where P is an integer, y_0 and y_* (also denoted as y_P) are the endpoints of the truncated interval for y. As an example, the rib waveguide shown in Fig. 1 has three horizontal interfaces ($P = 4$) even though there are only two physical interfaces in reach region. If we apply the Chebyshev pseudospectral method directly to Eqs. (5) and (6), we can choose the number of discretization points in each interval (y_{p-1}, y_p), but we cannot control how these points are distributed. To gain more flexibility, we introduce a coordinate transform given by $y = y(\xi)$ where ξ is a new variable and $y(\xi)$ is a piecewise-smooth and increasing function. Equations (5) and (6) become

$$\frac{\varepsilon}{s}\frac{d}{d\xi}\left(\frac{1}{\varepsilon s}\frac{d\phi}{d\xi}\right) + k_0^2 \varepsilon \phi = \hat{\delta}^2 \phi, \tag{15}$$

$$\frac{1}{s}\frac{d}{d\xi}\left(\frac{1}{s}\frac{d\psi}{d\xi}\right) + k_0^2 \varepsilon \psi = \hat{\nu}^2 \psi, \tag{16}$$

where $s = dy/d\xi$ is the derivative of y with respect to ξ. If the ξ value corresponding to y_p is ξ_p, i.e., $y_p = y(\xi_p)$ for $0 \le p \le P$, then boundary condition (7) is transformed to

$$\phi = \psi = 0 \quad \text{at} \quad \xi = \xi_0, \ \xi_*, \tag{17}$$

where $\xi_* = \xi_P$. This coordinate transform serves two purposes. It allows us to put more discretization points near waveguide corners where the electromagnetic field may be singular. For the rib waveguide shown in Fig. 1, the corners are located at (x_l, y_2) and (x_l, y_3) for $l = 1, 2$. Therefore, it could be beneficial to increase the density of discretization points near y_2 and y_3. When applied in the first and last intervals, i.e., (y_0, y_1) and (y_{P-1}, y_P), this coordinate transform also allows us to use a large computational window for y without increasing the total number of discretization points. This would be useful for computing waveguide modes that decay slowly as $|y| \to \infty$.

More specifically, we implement a coordinate transform satisfying $\xi_p = y_p$ for $1 \le p < P$, but $y_0 < \xi_0$ and $\xi_* < y_*$. On the interval (ξ_{p-1}, ξ_p) for $1 < p < P$, we follow the adaptive spatial resolution technique for Fourier modal method [41], and use the transform

$$y(\xi) = y_{p-1} + (y_p - y_{p-1}) \left[\tau - \frac{\eta_p}{2\pi} \sin(2\pi\tau) \right], \tag{18}$$

where

$$\tau = (\xi - \xi_{p-1})/(\xi_p - \xi_{p-1})$$

and η_p is a real parameter less than 1. To increase the density of discretization points around the two endpoints, we can choose a η_p close to 1. The first and last intervals are first expanded by

$$\hat{\xi} = \xi - S_0 \left(\frac{\xi_1 - \xi}{\xi_1 - \xi_0} \right)^3, \quad \xi_0 \le \xi \le \xi_1, \tag{19}$$

$$\hat{\xi} = \xi + S_* \left(\frac{\xi - \xi_{P-1}}{\xi_* - \xi_{P-1}} \right)^3, \quad \xi_{P-1} \le \xi \le \xi_* \tag{20}$$

for some positive constants S_0 and S_*, such that

$$\hat{\xi}_0 = \xi_0 - S_0 = y_0, \quad \hat{\xi}_* = \xi_* + S_* = y_*,$$

then Eq. (18) is applied with a revised τ defined by $\hat{\xi}$. That is,

$$\tau = \begin{cases} (\hat{\xi} - \hat{\xi}_0)/(\xi_1 - \hat{\xi}_0), & p = 1, \\ (\hat{\xi} - \xi_{P-1})/(\hat{\xi}_* - \xi_{P-1}), & p = P. \end{cases}$$

The new variable ξ is discretized in each interval $[\xi_{p-1}, \xi_p]$ separately as

$$\xi_{p,k} = \xi_{p-1} + \frac{\xi_p - \xi_{p-1}}{2}\left(1 - \cos\frac{k\pi}{q_p}\right), \ 0 \le k \le q_p, \quad (21)$$

where q_p is a positive integer. Notice that $\xi_{p,0} = \xi_{p-1}$ and $\xi_{p,q_p} = \xi_p$ are the endpoints of the interval. The Chebyshev pseudospectral method approximates the eigenvalue problems (15), (16) and (17) by matrix eigenvalue problems. For (15) and (17), the matrix approximation is

$$\mathbf{A}\begin{bmatrix} \boldsymbol{\phi}_1 \\ \boldsymbol{\phi}_2 \\ \vdots \\ \boldsymbol{\phi}_P \end{bmatrix} = \hat{\delta}^2 \begin{bmatrix} \boldsymbol{\phi}_1 \\ \boldsymbol{\phi}_2 \\ \vdots \\ \boldsymbol{\phi}_P \end{bmatrix}, \quad (22)$$

where $\boldsymbol{\phi}_p$ is a column vector for ϕ at the interior discretization points of (ξ_{p-1}, ξ_p), i.e., at $\xi_{p,k}$ for $1 \le k < q_k$, and $\mathbf{A}$ is an $N \times N$ matrix where

$$N = (q_1 - 1) + (q_2 - 1) + \cdots = \sum_{p=1}^{P} q_p - P.$$

Notice that the interface points ξ_p for $1 \le p < P$ are excluded in the matrix eigenvalue problem. In fact, Eq. (22) corresponds to Eq. (15) at the N collocation points $\xi_{p,k}$ for $1 \le p \le P$ and $1 \le k < q_p$.

The steps that give rise to the matrix $\mathbf{A}$ can be found in our earlier work [37]. Here we only emphasize two important aspects of the method. Firstly, there is a matrix $\mathbf{C}_p$ (Chebyshev differentiation matrix) that approximates the derivative operator on $[\xi_{p-1}, \xi_p]$. Let ϕ' be the derivative of ϕ with respect to ξ, then

$$\begin{bmatrix} \phi'(\xi_{p,0}^+) \\ \phi'(\xi_{p,1}) \\ \vdots \\ \phi'(\xi_{p,q_p-1}) \\ \phi'(\xi_{p,q_p}^-) \end{bmatrix} \approx \mathbf{C}_p \begin{bmatrix} \phi(\xi_{p,0}) \\ \phi(\xi_{p,1}) \\ \vdots \\ \phi(\xi_{p,q_p-1}) \\ \phi(\xi_{p,q_p}) \end{bmatrix}, \quad (23)$$

Secondly, we need to enforce the continuity of $(\varepsilon s)^{-1}\phi'$ at ξ_p for $1 \le p < P$. This gives rise to a linear equation relating ϕ at the interface points with ϕ at the N interior points, i.e.,

$$\begin{bmatrix} \phi(\xi_1) \\ \phi(\xi_2) \\ \vdots \\ \phi(\xi_{P-1}) \end{bmatrix} \approx \mathbf{B} \begin{bmatrix} \boldsymbol{\phi}_1 \\ \boldsymbol{\phi}_2 \\ \vdots \\ \boldsymbol{\phi}_P \end{bmatrix}, \quad (24)$$

where $\mathbf{B}$ is a $(P-1) \times N$ matrix.

When the matrix eigenvalue problem (22) is solved, we can use Eq. (24) to find the eigenfunctions at the interface points and use Eq. (23) to find the derivative of the eigenfunctions. The expansions (8), (9), (13) and (14) are replaced by their numerical versions where ϕ_j, ψ_j, $d\phi_j/dy = s^{-1}d\phi/d\xi$ and $d\psi_j/dy = s^{-1}d\psi/d\xi$ become column vectors of length N, and j ranges from 1 to N. When the four field components are matched at x_l ($1 \le l \le l_*$) and $\xi_{p,k}$ ($1 \le p \le P$, $1 \le k < q_p$), we obtain Eq. (1). Notice that $\mathbf{F}$ is a $(4l_*N) \times (4l_*N)$ matrix.

If the waveguide has a horizontal reflection symmetry, we can reduce the size of matrix $\mathbf{F}$ to $(2l_*N) \times (2l_*N)$ by considering waveguide modes with different symmetries separately. For the rib waveguide shown in Fig. 1, we can set the y-axis at the center of the structure (thus, $x_1 = -x_2$), and consider modes with even E_y and odd H_y, or odd E_y and even H_y. For the case of even E_y and odd H_y, the expansions (8) and (9) for the second region (i.e. $x_1 < x < x_2$) should be modified as

$$U_j(x) = a_j\left[e^{i\delta_j(x-x_1)} + e^{-i\delta_j(x-x_2)}\right], \quad (25)$$

$$V_j(x) = c_j\left[e^{i\nu_j(x-x_1)} - e^{-i\nu_j(x-x_2)}\right], \quad (26)$$

then the field components are only matched at x_1, giving rise to a $(4N) \times (4N)$ matrix $\mathbf{F}$ (since $l_* = 2$ for the rib waveguide).

To find β, we solve

$$\sigma_1(\mathbf{F}(\beta)) = 0 \quad (27)$$

by secant method or Müller's method, where $\sigma_1(\mathbf{F})$ is the smallest singular value of matrix $\mathbf{F}$.

In summary, our method involves the following steps:

1) divide the xy plane (perpendicular to the waveguide axis) into a number of regions where ε depends only on y (or x);
2) truncate y and choose parameters η_p, S_0 and S_* in (18), (19) and (20), respectively, for coordinate transform;
3) discretize the eigenvalue problems (15), (16) and (17);
4) find the derivatives of the eigenfunctions by Eq. (23);
5) establish the matrix $\mathbf{F}(\beta)$ from the continuity conditions at the interfaces between the regions;
6) solve β from Eq. (27) numerically;
7) for the found β, solve the vector $\boldsymbol{x}$ in Eq. (1) and construct the electromagnetic field from $\boldsymbol{x}$.

IV. Numerical examples

In this section, we present some numerical examples to validate and illustrate our method. The first example is a classical rib waveguide previously analyzed by a number of authors [1], [10], [12], [31], [44]. The cross section of the waveguide is shown in Fig. 1, where the rib width is $w = 3.0\,\mu$m, the rib thickness is $h = 1\,\mu$m, and the thickness of the slab is $t = 0.5\,\mu$m. The refractive indices of the cladding, the guiding layer and the substrate are $n_t = 1$, $n_c = 3.44$ and $n_b = 3.4$, respectively. As in the earlier works mentioned above, we assume the free space wavelength is $\lambda = 1.15\,\mu$m. For this waveguide, we use the PSMM without a coordinate transform. Assuming the horizontal interface between the substrate and the guiding layer is located at $y = y_1 = 0$, we truncate the y variable to (y_0, y_*) where $y_0 = -5\,\mu$m and $y_* = 2\,\mu$m. This

leads to four intervals of y given by (y_{p-1}, y_p) for $1 \le p \le 4$, where $y_2 = 0.5\,\mu$m, $y_3 = 1\,\mu$m and $y_4 = y_*$. In Table I, we show the computed normalized propagation constant β/k_0

TABLE I
NORMALIZED PROPAGATION CONSTANT β/k_0 OF A RIB WAVEGUIDE, OBTAINED BY THE PSMM FOR DIFFERENT VALUES OF N.

N	β/k_0	N	β/k_0
120	3.4131279877	360	3.4131321427
160	3.4131353849	400	3.4131321423
200	3.4131305520	440	3.4131321421
240	3.4131321477	480	3.4131321420
280	3.4131321441	520	3.4131321418
320	3.4131321433		

for different values of N. Notice that for $N = 240$ and 280, we obtain $\beta/k_0 \approx 3.4131321$ and $\beta/k_0 \approx 3.41313214$, respectively. These results contain 8 and 9 correct digits, respectively. Excellent agreement is obtained with the earlier results reported in [1], [10], [12].

The second example, shown in Fig. 2(a), is a square

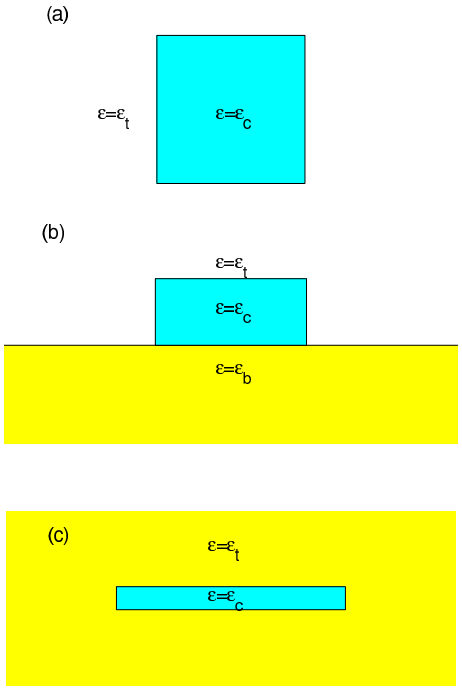

Fig. 2. Optical waveguides with high index-contrast: (a) a square dielectric waveguide; (b) a silicon wire on a silica substrate; (c) a plasmonic waveguide (silver strip surrounded by a dielectric medium).

waveguide previously analyzed by Hadley [1] and others [18], [22]. The waveguide has a $1\,\mu$m $\times$ $1\,\mu$m high-index dielectric core surrounded by air. The dielectric constants of the core and the surrounding medium are $\varepsilon_c = 8$ and $\varepsilon_t = 1$, respectively. The problem is considered for the free space wavelength $\lambda = 1.5\,\mu$m. For this waveguide, we assume the horizontal edges of the square core are located at $y = y_1$ and $y = y_2$, and truncate the y variable to (y_0, y_*) where $y_0 = -2\,\mu$m, $y_1 = 0$, $y_2 = 1\,\mu$m, and $y_* = y_3 = 3\,\mu$m. The discretization is carried out in the transformed variable ξ with $\xi_0 = -1\,\mu$m, $\xi_1 = y_1$, $\xi_2 = y_2$ and $\xi_* = \xi_3 = 2\,\mu$m. This corresponds to $S_0 = S_* = 1\,\mu$m in Eqs. (19) and (20). Formula (18) is used on all three intervals with $\eta_p = 0.99$. Our numerical results are listed in Table II. In [22], a very accurate result for

TABLE II
NORMALIZED PROPAGATION CONSTANT β/k_0 OF A SQUARE WAVEGUIDE, OBTAINED BY THE PSMM FOR DIFFERENT VALUES OF N.

N	β/k_0	N	β/k_0
60	2.6567749515	270	2.6567955306
90	2.6567954014	300	2.6567955306
120	2.6567955294	330	2.6567955306
150	2.6567955299	360	2.6567955307
180	2.6567955302	390	2.6567955307
210	2.6567955304	420	2.6567955307
240	2.6567955305	450	2.6567955307

this waveguide was obtained by a BIE method. Comparing with that, we conclude that the PSMM gives 9 correct digits ($\beta/k_0 \approx 2.65679553$) for $N = 120$ and 10 correct digits ($\beta/k_0 \approx 2.656795531$) for $N = 240$.

The third example, shown in Fig. 2(b), is a rectangular silicon waveguide on a silica substrate. The size of the rectangular core is $0.5\,\mu$m $\times$ $0.22\,\mu$m. The refractive indices of the core, the substrate and the cladding are $n_c = 3.5$, $n_b = 1.45$ and $n_t = 1$, respectively. The waveguide is analyzed for the free space wavelength $\lambda = 1.55\,\mu$m. Similar to the second example, we use the coordinate transform and discretize the y variable through ξ in three intervals. For the variable y, the interface and end points are $y_0 = -3.22\,\mu$m, $y_1 = 0$, $y_2 = 0.22\,\mu$m, $y_* = y_3 = 2.44\,\mu$m, where $y = 0$ is the horizontal interface between the core and the substrate. The corresponding points for ξ are $\xi_0 = -0.22\,\mu$m, $\xi_1 = 0$, $\xi_2 = 0.22\,\mu$m, $\xi_* = \xi_3 = 0.44\,\mu$m, and they are related by $S_0 = 3\,\mu$m and $S_* = 2\,\mu$m. Equation (18) is used on all intervals with $\eta_p = 0.99$. This waveguide has been previously analyzed by a BIE method [22]. Our results are given Table III. For $N = 240$, we obtain $\beta/k_0 \approx 2.41237199$, which

TABLE III
NORMALIZED PROPAGATION CONSTANT β/k_0 OF A SILICON WAVEGUIDE, OBTAINED BY THE PSMM FOR DIFFERENT N.

N	β/k_0	N	β/k_0
120	2.41149824	300	2.41237199
150	2.41243857	330	2.41237199
180	2.41236892	360	2.41237199
210	2.41237209	390	2.41237199
240	2.41237199	420	2.41237199
270	2.41237199		

perfectly agrees with the result of [22]. The adaptive spatial resolution technique is useful for this waveguide with a high index-contrast. In Table IV, we show the numerical results for

TABLE IV
NORMALIZED PROPAGATION CONSTANT β/k_0 OF A SILICON WAVEGUIDE, OBTAINED BY THE PSMM FOR DIFFERENT η_p AND $N = 240$.

η_p	β/k_0	η_p	β/k_0
0.99	2.41237199	0.4	2.41237207
0.9	2.41237200	0.3	2.41237208
0.8	2.41237202	0.2	2.41237209
0.7	2.41237203	0.1	2.41237211
0.6	2.41237204	0	2.41237212
0.5	2.41237205		

different values of η_p at the fixed $N = 240$. A descrease of accuracy can be observed as η_p is decreased to 0.

Finally, we consider a plasmonic waveguide previously studied by Berini [45]–[47]. The waveguide, shown in Fig. 2(c), has a silver core of size $1\,\mu\text{m} \times 0.1\,\mu\text{m}$ and it is surrounded by a homogeneous medium. The waveguide is considered for the free space wavelength $\lambda = 0.633\,\mu\text{m}$. For this wavelength, the dielectric constant of silver is $\varepsilon_c = -19 + 0.53i$, and the dielectric constant of the surrounding medium is assumed to be $\varepsilon_t = 4$. For the PSMM, we use the coordinate transform $y = y(\xi)$ as in the previous two examples. The two sets of interface and end points are $y_0 = -0.7\,\mu\text{m}$, $\xi_0 = -0.1\,\mu\text{m}$, $y_1 = \xi_1 = 0$, $y_2 = \xi_2 = 0.1\,\mu\text{m}$, $\xi_3 = 0.2\,\mu\text{m}$, $y_3 = 0.8\,\mu\text{m}$, and they are related by $S_0 = S_* = 0.6\,\mu\text{m}$. For Eq. (18), the parameter is $\eta_p = 0.99$. In Table V, we show the numerical results obtained by the PSMM for two guided modes. For the first mode, we get $\beta_1/k_0 \approx 2.84153 + i3.896 \times 10^{-2}$ for $N = 180$. The second mode is more difficult to calculate. For $N = 330$, we obtain the solution $\beta_2/k_0 \approx 2.38010 + i2.796 \times 10^{-2}$. For both modes, our results agree well with the those of [47].

TABLE V
COMPLEX NORMALIZED PROPAGATION CONSTANTS OF TWO GUIDED MODES OF A PLASMONIC WAVEGUIDE, OBTAINED BY THE PSMM.

N	β_1/k_0	β_2/k_0
120	2.8395448+3.889923E-2i	2.3791031+2.788329E-2i
150	2.8415705+3.896168E-2i	2.3801346+2.796572E-2i
180	2.8415314+3.896016E-2i	2.3801092+2.796284E-2i
210	2.8415330+3.895969E-2i	2.3801079+2.796207E-2i
240	2.8415333+3.895931E-2i	2.3801067+2.796151E-2i
270	2.8415333+3.895900E-2i	2.3801057+2.796109E-2i
300	2.8415332+3.895875E-2i	2.3801050+2.796078E-2i
330	2.8415331+3.895856E-2i	2.3801044+2.796053E-2i
360	2.8415329+3.895839E-2i	2.3801040+2.796033E-2i
390	2.8415327+3.895825E-2i	2.3801036+2.796017E-2i
420	2.8415325+3.895814E-2i	2.3801033+2.796004E-2i
450	2.8415324+3.895804E-2i	2.3801030+2.795993E-2i
480	2.8415323+3.895795E-2i	2.3801028+2.795983E-2i

V. CONCLUSION

In this paper, the pseudospectral modal method (PSMM), previously developed for analyzing diffraction gratings, is reformulated as a full-vectorial optical waveguide mode solver. The method can be regarded as a numerical variant of the classical mode-matching method [23]–[28]. Since it simply solves the related 1D modes numerically by the standard Chebyshev pseudospectral method, the PSMM is easy to implement. The classical mode-matching method can be difficult to use for waveguides with lossy components, since it requires a systematic method for locating zeros of transcendental functions in the complex plane (for analytic solutions of the 1D modes). We also implement a coordinate transform for the PSMM, which can be used to increase the density of discretization points near material interfaces or waveguide corners, and to expand the domain of truncation without increasing the total number of points. Numerical examples in Section IV indicate that the PSMM gives accurate solutions for waveguides with high index-contrast and right-angle corners.

REFERENCES

[1] G. R. Hadley, "High-accuracy finite-difference equations for dielectric waveguide analysis II: Dielectric cornors," *J. Lightwave Technol.*, vol. 20, pp. 1219-1231, 2002.

[2] M. Wik, D. Dumas, and D. Yevick, "Comparison of vector finite-difference techniques for modal analysis," *J. Opt. Soc. Am. A*, vol. 22, pp. 1341-1347, 2005.

[3] N. Thomas, P. Sewell, and T. M. Benson, "A new full-vectorial higher order finite-difference scheme for the modal analysis of rectangular dielectric waveguides," *J. Lightwave Technol.*, vol. 25, pp. 2563-2570, 2007.

[4] Y. P. Chiou, Y. C. Chiang, C. H. Lai, C. H. Du, and H. C. Chang, "Finite difference modeling of dielectric waveguides with corners and slanted facets," *J. Lightwave Technol.*, vol. 27, pp. 2077-2086, 2009.

[5] B. M. A. Rahman and J. B. Davies, "Finite-element solution of integrated optical wave-guides," *J. Lightwave Technol.*, vol. 2, pp. 682-688, 1984.

[6] M. Koshiba, K. Hayata, and M. Suzuki, "Vectorial finite-element method without spurious solutions for dielectric waveguide problems", *Electron. Lett.*, vol. 20, pp. 409-410, 1984.

[7] Z. E. Abid, K. L. Johnson, and A. Gopinath, "Analysis of dielectric guides by vector transverse magnetic field finite elements," *J. Lightwave Technol.*, vol. 11, pp. 1545-1549, 1993.

[8] S. Selleri, L. Vincetti L, A. Cucinotta, and M. Zoboli, "Complex FEM modal solver of optical waveguides with PML boundary conditions," *Opt. Quant. Electron.*, vol. 33, pp. 359-371, 2001.

[9] C. C. Huang, C. C. Huang, and J. Y. Yang, "A full-vectorial pseudospectral modal analysis of dielectric optical waveguides with stepped refractive index profiles," *IEEE J. Sel. Top. Quantum Electron.*, vol. 11, pp. 457-465, 2005.

[10] P. J. Chiang, C. L. Wu, C. H. Teng, C. S. Yang, and H. C. Chang, "Full-vectorial optical waveguide mode solvers using multidomain pseudospectral frequencydomain (PSFD) formulations," *IEEE J. Quantum Electron.*, vol. 44, pp. 56-66, 2008.

[11] S. F. Chiang, B. Y. Lin, H. C. Chang, C. H. Teng, C. Y. Wang, and S. Y. Chung, "A multidomain pseudospectral mode solver for optical waveguide analysis," *J. Lightwave Technol.*, vol. 30, pp. 20772087, July 2012.

[12] C. Y. Wang, H. H. Liu, S. Y. Chung, C. H. Teng, C. P. Chen, and H. C. Chang, "High-accuracy waveguide leaky-mode analysis using a multidomain pseudospectral frequency-domain method incorporated with stretched coordinate PML," *J. Lightwave Technol.*, vol. 31, pp. 2347-2360, July 2013.

[13] K. M. Lo, R. C. McPhedran, I. M. Bassett, and G. W. Milton, "An electromagnetic theory of dielectric waveguides with multiple embedded cylinders," *J. Lightwave Technol.*, vol. 12, pp. 396-410, 1994.

[14] C. S. Chang and H. C. Chang, "Theory of the circular harmonics expansion method for multiple-optical-fiber system," *J. Lightwave Technol.*, vol. 12, pp. 415-417, 1994.

[15] T. P. White, B. T. Kuhlmey, R. C. McPhedran, D. Maystre, G. Renversez, C. M. de Sterke, and L. C. Botten, "Multipole method for microstructured optical fibers I: Formulation," *J. Opt. Soc. Am. B*, vol. 19, pp. 2322-2330, 2002.

[16] B. T. Kuhlmey, T. P. White, G. Renversez, D. Maystre, L. C. Botten, C. M. de Sterke, and R. C. McPhedran, "Multipole method for microstructured optical fibers II: Implementation and results," *J. Opt. Soc. Am. B*, vol. 19, pp. 2331-2340, 2002.

[17] S. V. Boriskina, T. M. Benson, P. Sewell, and A. I. Nosich, "Highly efficient full-vectorial integral equation solution for the bound, leaky, and complex modes of dielectric waveguides," *IEEE J. Sel. Top. Quantum Electron.*, vol. 8, pp. 1225-1232, 2002.

[18] T. Lu and D. Yevick, "Comparative evaluation of a novel series approximation for electromagnetic fields at dielectric corners with boundary element method applications," *J. Lightwave Technol.*, vol. 22, pp. 1426-1432, 2004.

[19] H. Cheng, W. Y. Crutchfield, M. Doery, and L. Greengard, "Fast, accurate integral equation methods for the analysis of photonic crystal fibers I: theory," *Opt. Express*, vol. 12, pp. 3791-3805, 2004.

[20] E. Pone, A. Hassani, S. Lacroix, A. Kabashin, and M. Skorobogatiy, "Boundary integral method for the challenging problems in bandgap guiding, plasmonics and sensing," *Opt. Express*, vol. 15, pp. 10231-10246, 2007.

[21] W. Lu and Y. Y. Lu, "Efficient boundary integral equation method for photonic crystal fibers," *J. Lightwave Technol.*, vol. 20, pp. 1610-1616, June 2012.

[22] W. Lu and Y. Y. Lu, "Waveguide mode solver based on Neumann-to-Dirichlet operators and boundary integral equations," *J. Comput. Phys.*, vol. 231, pp. 1360-1371, 2012.

[23] K. Solbach and I. Wolff, "The electromagnetic fields and the phase constants of dielectric image lines," *IEEE Trans. Microwave Theory Tech.*, vol. 26, pp. 266-274, April 1980.

[24] R. Mittra, Y. L. Hou, and V. Jamnejad, "Analysis of open dielectric wave-guides using mode-matching technique and variational-methods," *IEEE Trans. Microwave Theory Tech.*, vol. 28, pp. 36-43, 1980.

[25] S. T. Peng and A. A. Oliner, "Guidance and leakage properties of a class of open dielectric waveguides: part I – mathematical formulations," *IEEE Trans. Microwave Theory Tech.*, vol. 29, pp. 843-855, Sept. 1981.

[26] A. S. Sudbo, "Numerically stable formulation of the transverse resonance method for vector mode-field calculations in dielectric waveguides," *IEEE Photon. Technol. Lett.*, vol. 5, pp. 342-344, 1993.

[27] A. S. Suddo, "Film mode matching: a versatile numerical method for vector mode field calculations in dielectric waveguides," *Pure Appl. Opt.*, vol. 2, pp. 211-233, 1993.

[28] P. Bienstman, "Two-stage mode finder for waveguides with a 2D cross-section," *Opt. Quant. Electron.*, vol. 36, pp. 5-14, 2004.

[29] L. Prkna, M. Hubálek, and J. Ctyroky, "Vectorial eigenmode solver for bent waveguides based on mode matching," *IEEE Photon. Technol. Lett.*, vol. 16, pp. 2057-2059, Sept. 2004.

[30] U. Rogge and R. Pregla, "Method of lines for the analysis of dielectric waveguides," *J. Lightwave Technol.*, vol. 11, pp. 2015-2020, Dec. 1993.

[31] J. P. Hugonin, P. Lananne, I. Delvillar, and I. R. Matias, "Fourier modal methods for modeling optical dielectric waveguides," *Opt. Quant. Electron.*, vol. 31, pp. 107-119, 2005.

[32] P. Debackere, P. Bienstman, and R. Baets, "Adaptive spatial resolution: application to surface plasmon waveguide modes," *Opt. Quant. Electron.*, vol. 38, pp. 857-867, 2006.

[33] P. Bienstman, S. Selleri *et al.* "Modelling leaky photonic wires: A mode solver comparison," *Opt. Quant. Electron.*, vol. 38, pp. 731-759, 2006.

[34] L. Li, "A modal analysis of lamellar diffraction gratings in conical mountings," *J. Mod. Opt.*, vol. 40, pp. 553-573, 1993.

[35] D. Song and Y. Y. Lu, "High order finite difference modal method for diffraction gratings," *J. Mod. Opt.*, vol. 59, no. 9, pp. 800-808, May 2012.

[36] Y.-P. Chiou, W.-L. Yeh, and N.-Y. Shih, "Analysis of highly conducting lamellar gratings with multidomain pseudospectral method," *J. Lightwave Technol.*, vol. 27, pp. 5151-5159, 2009.

[37] D. Song, L. Yuan, and Y. Y. Lu, "Fourier-matching pseudospectral modal method for diffraction gratings," *J. Opt. Soc. Am. A*, vol. 28, pp. 613-620, 2011.

[38] G. Granet, "Fourier-matching pseudospectral modal method for diffraction gratings: comment," *J. Opt. Soc. Am. A*, vol. 29, pp. 1843-1845, 2012.

[39] D. Song, L. Yuan, and Y. Y. Lu, "Fourier-matching pseudospectral modal method for diffraction gratings: reply," *J. Opt. Soc. Am. A*, vol. 29, pp. 1846, 2012.

[40] D. Song and Y. Y. Lu, "Pseudospectral modal method for conical diffraction of gratings," *J. Mod. Opt.*, vol. 60, pp. 1729-1734, 2013.

[41] G. Granet, "Reformulation of the lamellar grating problem through the concept of adaptive spatial resolution," *J. Opt. Soc. Am. A*, vol. 16, pp. 2510-2516, 1999.

[42] T. Vallius and M. Honkanen, "Reformulation of the Fourier modal method with adaptive spatial resolution: application to multilevel profiles," *Opt. Express*, vol. 10, pp. 24-34, 2002.

[43] L. N. Trefethen, *Spectral Methods in MATLAB*, Society for Industrial and Applied Mathematics, 2000.

[44] C. Vassallo, "1993-1995 optical mode solvers," *Opt. Quant. Electron.*, vol. 29, pp. 95-114, 1997.

[45] P. Berini, "Plasmon-polariton modes guided by a metal film of finite width," *Opt. Lett.*, vol. 24, pp. 1011-1013, 1999.

[46] P. Berini, "Plasmon-polariton waves guided by thin lossy metal films of finite width: Bound modes of symmetric structures," *Phys. Rev. B*, vol. 61, pp. 10484-10503, 2000.

[47] P. Berini and R. Buckley, "On the convergence and accuracy of numerical mode computations of surface plasmon waveguides," *J. Comput. Theor. Nanos.*, vol. 6, pp. 2040-2053, 2009.